Materials and Design 186 (2020) 108352

Contents lists available at ScienceDirect

Materials and Design

journal homepage: www.elsevier.com/locate/matdes

Novel view at hybrid membranes containing star macromolecules using neutron scattering and pervaporation dehydration of acetic acid

Galina Polotskaya [a,b], Alexandra Pulyalina [b,*], Vasily Lebedev [c], Gyula Török [d], Daria Rudakova [b], Ludmila Vinogradova [a]

[a] Institute of Macromolecular Compounds, Russian Academy of Sciences, 199004 Saint Petersburg, Russia
[b] Saint Petersburg State University, Institute of Chemistry, 198504 Saint Petersburg, Russia
[c] B.P. Konstantinov Saint Petersburg Nuclear Physics Institute, NRC «Kurchatov Institute», 188300 Leningradskaya Oblast, Gatchina, Russia
[d] Research Institute for Solid State Physics and Optics, Wigner Research Centre for Physics, Hungarian Academy of Sciences, Budapest, Hungary

HIGHLIGHTS

- Polyphenylene oxide was modified by star macromolecules with different natures of arms for membrane preparation
- The effect of star modifiers on membrane structure, density, surface, sorption and separation parameters was investigated
- Membranes structure was studied by small-angle neutron scattering method for mass transfer characterization
- Star macromolecules create an additional free volume which affects on pervaporation performance
- The water impurities were effectively removed from acetic acid using hybrid membranes containing up to 5 wt% of modifiers

GRAPHICAL ABSTRACT

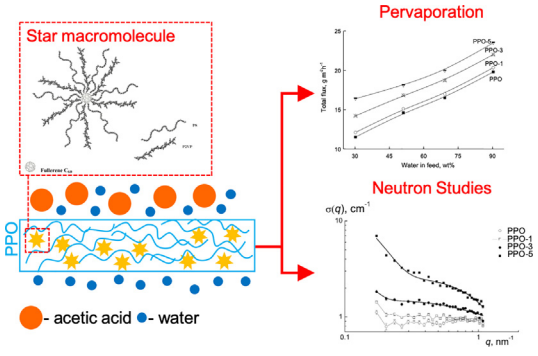

ARTICLE INFO

Article history:
Received 18 September 2019
Received in revised form 10 November 2019
Accepted 11 November 2019
Available online 13 November 2019

Keywords:
Pervaporation
Neutron scattering
Membrane
Polyphenylene oxide
Star macromolecules
Acetic acid – water mixture

ABSTRACT

Hybrid membranes based of polyphenylene oxide matrix and star macromolecules (up to 5 wt%) containing six polystyrene and six poly-2-vinylpyridine arms attached to a common fullerene C_{60} center were prepared and successfully used for pervaporation separation of acetic acid – water mixtures. The peculiarities of the hybrid membrane structure and properties were studied by small-angle neutron scattering in two states (dry and swollen in deuterated acetic acid). It was established that star macromolecules are non-uniformly distributed in the matrix and form aggregates; they increase in the size up to ~60% during swelling of membranes in deuterated acetic acid. In pervaporation, the total flux through the membrane rises with increasing both the star macromolecule content in membrane and water concentration in the feed. Separation factor reaches its greatest value when the hybrid membrane contains 5 wt% star macromolecules.

* Corresponding author.
E-mail address: a.pulyalina@spbu.ru (A.x Pulyalina).

https://doi.org/10.1016/j.matdes.2019.108352

1. Introduction

Modern membrane technologies have great potential for applications in separation, concentration, and purification of substances in the liquid and gaseous states [1,2]. Acetic acid is among the most important products of commercial organic synthesis. Only a small portion of the produced acetic acid is used in the home and food industry; the bulk of the product is consumed in chemical and pharmaceutical industries, in the processing of synthetic fibers and fabrics, printing, leather industry, paint and varnish industry, etc. More than half of all acetic acid manufactured in the world is spent on synthesis of polymers (namely, cellulose and vinyl acetate derivatives). World production and consumption of acetic acid is growing steadily every year. According to the forecasts made by Global Industry Analytics, Inc. (Acetic Acid - Market Analysis, Trends and Forecasts), consumption of acetic acid will reach 20.2 million metric tons by 2024.

Anhydrous (glacial) acetic acid is often necessary for performing various reactions. Acetic acid and water do not form mixtures of azeotropic composition, however, the separation of the components of these mixtures is difficult. Dehydration of acetic acid containing 3–5 wt% of water can be performed using water bonding agents (sodium and magnesium sulfates, phthalic anhydride, calcium chloride, etc.), as well as by azeotropic distillation in the presence of *n*-propyl or *n*-butyl acetate (the entrainers that form azeotropes with water) [3].

An alternative method for separation of acetic acid – water mixtures is membrane pervaporation; advantages of this technique include resource saving, low energy consumption, smaller capital investment, enhanced ease of operation and high productivity [4–8]. In contrast to rectification process, pervaporation membranes separate mixtures at mild temperatures and without the introduction of additional components even for separation of azeotropic mixtures and close boiling liquids. Pervaporation efficiency depends on the type of the selected membrane material. Various chemically modified polymers were studied as membrane materials in dehydration of acetic acid; they include copolymers, graft-copolymers, cross-linked polymers or composites based on polyacrylonitrile [9–11], poly(vinyl alcohol) [12–14], polysulfone [15], nylon-6 [16,17], polybenzimidazole [18] and mixed matrix membranes filled with particles of different type (silicate [19], zeolites [20,21], fullerenol [22], montmorillonite [23]). To solve the problems of separating acetic acid – water mixtures, acid-resistant silicalite and organosilica membranes were developed [24–26], as well as zeolite-based membranes with surface layer consisting of graphene oxide [27]. Notice also the membranes for separation of acetic acid and water produced in the form of multicomponent polymer systems that were subjected to additional modification [28,29] and composite membranes in the form of polymer layers fixed on micro- and ultraporous substrates [30,31]. Preparation of the above-mentioned membranes involves a number of experimental difficulties (such as synthesis of the polymers with complex structure, additional chemical modification of the membrane or its selective layer, multi-stage synthesis, and formation of the membrane, etc.).

The singularity of the present work is the use one of the simplest methods for modifying membranes that consists in physical combination of matrix poly(2,6-dimethyl-1,4-phenylene oxide) (PPO) and a modifier by mixing solutions of the components followed by removal of the solvent. PPO membranes have not yet been applied for separation of acetic acid – water mixtures. PPO has proven itself as a suitable material for producing diffusion membranes due to its good mechanical strength, high thermal stability, chemical and radiation resistance [32,33]. PPO membranes were modified by various carbon or mineral nanoparticles to improve their transport properties [34–38].

In our previous works, pervaporation membranes have been modified by small amounts of star macromolecules (1–5 wt%) [39–41]. Six-arm or twelve-arm stars consisted of fullerene C_{60} core, polystyrene (PS) arms [39] and polymeric arms of different nature [40,41]. These membranes were used in pervaporation of methanol – ethylene glycol mixture and separation of a quaternary mixture (*n*-propanol – acetic acid – propyl acetate – water). The increase in modifier content up to 5 wt% led to an enhancement of efficiency of methanol purification; equilibrium of esterification reaction shifted, and the ester yield increased.

The main goal of the present work was to study transport properties of PPO membranes modified by small amounts of star macromolecules with C_{60} core in pervaporation separation of acetic acid – water mixture. The star macromolecule consisted of a fullerene C_{60} core with six attached nonpolar PS arms and six arms of polar poly-2-vinylpyridine (P2VP). Small-angle neutron scattering was used to study changes in the structure of the membranes modified by star macromolecules that occur during swelling in deuterated acetic acid. This method enables one to investigate films in the dry and swollen state using selective isotopic contrast (swelling in a deuterated solvent). Besides, small-angle neutron scattering provides an opportunity to study fine structural features of a membrane (morphological formations, micro (nano) cavities), which cannot be registered by electron microscopy and other methods.

Small-angle neutron scattering has been used in our previous works [42–44]. It has been shown that introducing star macromolecules into PPO matrix leads to appearance of changes in membrane structure, formation of regions with different polymer packing densities, variations in the arrangement of macromolecules.

2. Experimental

2.1. Materials

Poly(phenylene oxide) (molecular weight: 172 kDa, density: 1.057 g cm^{-3}, Brno, Czech Republic) and fullerene C_{60} (purity: 99.9%, Neo Tech Product, Research&Production Company, Russia) were used. Chloroform (Vecton, Russia) was used as a solvent without additional purification. Nonporous cellophane film (thickness: 70 μm) based on cellulose hydrate (Secon, Germany) was used as a support.

Star macromolecules (Fig. 1) were obtained by attaching chains of different structure (polystyrene and poly-2-vinylpyridine) to the fullerene C_{60} core; in this process, anionic polymerization methods were used [45,46].

In the resulting twelve-arm star macromolecule, the C_{60} core carries equal numbers of PS and P2VP arms. The structure of regular twelve-arm star macromolecule has been proven earlier by hydrodynamic studies. [47]. According to the data of size-exclusion chromatography, molecular weight of PS arm was $M_n = 6900$ D ($M_w/M_n = 1.04$). The length of P2VP arm was predetermined by polymerization conditions so as to be equal to the length of the non-polar arm; the experimentally estimated value was 7000 D [45,46].

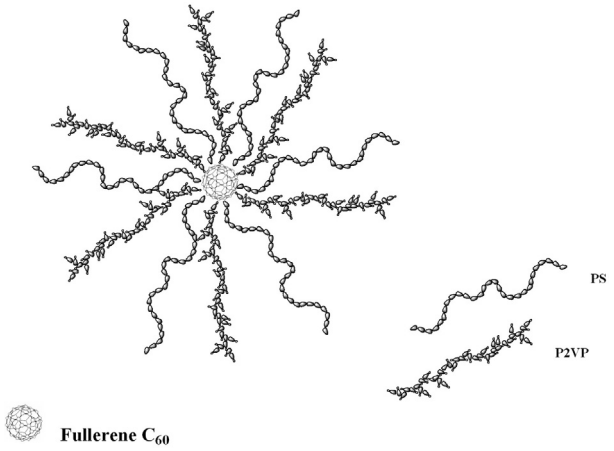

Fig. 1. Schematic representation of star macromolecule.

2.2. Membrane preparation

The PPO-based composites containing 1, 3, and 5 wt% star macromolecules (denoted as PPO-0, PPO-1, PPO-3, and PPO-5, respectively) were prepared by mixing measured amounts of 3 wt% solution of PPO and 3 wt% solution of the star modifier in chloroform. The mixed solutions were stirred intensely for 1 h and kept under steady state conditions for 2–3 days in order for interaction between PPO and star macromolecules to occur at room temperature. Finally, the solutions were sonicated for 40 min to achieve uniform distribution of star filler.

Thin film membranes were obtained by casting 3 wt% polymer solutions in chloroform onto nonporous cellophane support. The solvent was removed by evaporation at 40 °C for 24 h. The membrane was separated from the substrate and dried in a vacuum oven at 60 °C (pressure 2 mbar) until constant weight was reached (about 3 weeks).

2.3. Membrane characterization

Film density ρ (g cm^{-3}) was estimated by the flotation method using a laboratory-made measurement unit and water - saccharose solutions. The weight of used samples was 0.05–0.10 g; the error of measurements was ± 0.0001 g cm^{-3}.

Contact angles were measured by sessile drop method with the aid of the Drop Shape Analyzer DSA 10 (KRÜSS, Germany) under atmospheric pressure, at 20 °C. Water was used as a test liquid (surface tension 72.4 mN/m).

2.4. Neutron studies

To perform neutron scattering experiments, the films were cut into strips (10 × 60 mm), and these strips (4–6 films) were stacked together to obtain the layers 0.30–0.70 mm thick. The measurements were carried out at ambient temperature (20 °C) and involved dry and swollen film samples. The "Yellow submarine" diffractometer (BNC, Budapest, Hungary) was used in the experiments; scattering was detected in the range of momentum transfer $q = (4\pi/\lambda)\sin(\theta/2) = 0.08$–$4.5\ nm^{-1}$ (θ is the scattering angle, λ is the neutron wavelength (0.386 nm and 0.751 nm), full spectral width at half maximum is $\Delta\lambda/\lambda \approx 0.1$). The data corrected for background scattering were normalized to the intensities (I_W) measured for the standard (light water, layer thickness d_W = 1 mm) with the known cross section $d\sigma_W(q)/d\Omega$ per unit solid angle (Ω) and unit volume (cm^3). This procedure enables one to take into account the efficiency of detector cells and obtain the differential cross sections of the samples in absolute units, $d\sigma(q)/d\Omega = (I_S/I_W)(d_W/d_S)\, d\sigma_W(q)/d\Omega$, per unit solid angle and unit sample volume. Before and after scattering measurements, the transmissions (Tr) of the samples for neutron beam were controlled. The Tr magnitude depends on film thickness and density as well as the presence of a solvent inside a sample.

First, the structure of dry PPO films and its composites with star macromolecules was studied. Then these samples were saturated with deuterated acetic acid during ~10 h, since this solvent has a good contrast against polymer matrix [48]. Finally, the data obtained for dry and wet films were compared.

Sorption experiments were performed by immersion of membrane samples into individual liquid (acetic acid or water) at atmospheric pressure, 50 °C. After a while, samples were removed from the liquid, wiped carefully with tissue paper and weighed immediately; the error was $\pm 10^{-4}$ g. The experiment was continued until sorption equilibrium was reached.

The degree of equilibrium sorption, S (g liquid/100 g polymer), was calculated by the following equation:

$$S = \frac{M_s - M_d}{M_d} \cdot 100 \quad (1)$$

where M_s is the weight of a swollen membrane in equilibrium state, and M_d is the weight of a dry membrane.

2.5. Pervaporation

Membrane transport properties were evaluated using the setup for vacuum pervaporation with the effective membrane area of 14.8 cm^2 at 50 °C. The downstream pressure was maintained below 10^{-2} mmHg. Under these conditions, the stationary flow was established in 5–6 h, and the membranes demonstrated stable performance for a month. A non-flow stainless steel cell equipped with a stirrer was used. The permeate was collected into a liquid nitrogen cooled trap, weighed and analyzed. Permeate composition was determined using a Chromatec–Crystal 5000.2 chromatograph (Chromatec, Russia) equipped with a thermal conductivity detector and a Porapak Q column (80/100 mesh).

Separation factor was calculated by the following equation:

$$\alpha = (Y_{Water}/Y_{HAc})/(X_{Water}/X_{HAc}) \quad (2)$$

where Y_{Water} and Y_{HAc} are the weight fractions of water and acetic acid in the permeate, and X_{Water} and X_{HAc} are the weight fractions of water and acetic acid in the feed.

Membrane flux, $J\ (g\ m^{-2}\ h^{-1})$, was determined as an amount of liquid penetrated through membrane area per unit time. To compare permeability of membranes with different thicknesses l (varied from 18 to 26 μm), the normalized permeability value J_n was used. J_n is the permeability through membrane with a thickness of 20 μm calculated as: $J_n = J \cdot l/20$.

To estimate intrinsic properties of a penetrant – membrane system, permeability and selectivity were calculated [49]. Membrane permeability (P_i) can be determined as a flux of a component normalized to membrane thickness and driving force; it was calculated using the following equation:

$$P_i = j_i \frac{l}{p_{i0} - p_{il}} \quad (3)$$

where j_i is the molar flux of component i (cm^3 (STP)/cm^2 s), and p_{i0} and p_{il} are the partial pressures of component i on both sides of the membrane (0 stands for the surface on the feed side, and l stands for the surface on the permeate side). Permeability was expressed in Barrer units (1 Barrer = $1 \cdot 10^{-10}$ (cm^3 (STP)·cm/cm^2 s·cm Hg).

In order to maintain the driving force of separation, a vacuum was created on the permeate side of the membrane; therefore, the partial pressures were equal to zero here.

Partial pressures of components on the feed side were calculated using components activities, which were taken from [50].

Membrane selectivity $\beta_{Water/HAc}$ was defined as a ratio between permeabilities:

$$\beta_{Water/HAc} = P_{Water}/P_{HAc} \quad (4)$$

3. Results and discussion

Hybrid membranes were prepared from the composites based on poly(phenylene oxide) (PPO) and star macromolecules with C_{60} core; the composites contained 1, 3, and 5 wt% star modifier and were denoted as PPO-0, PPO-1, PPO-3, and PPO-5, respectively. The membranes were used in pervaporation and small-angle neutron scattering experiments. The properties of hybrid membranes differ significantly from those of the matrix polymer. Introduction of the star modifier that consists of fullerene C_{60} core with six attached PS arms and six P2VP arms into the PPO matrix results in changes in physical properties of the membranes (such as glass transition temperature, density, and contact

angle [41]). As seen from Table 1, the values of glass transition temperature and densities of membranes increase with increasing star filler content in the PPO matrix. These phenomena are attributed to strengthening of intermolecular interactions between the matrix polymer and the star filler and to a certain decrease in chain mobility. The membrane structure becomes more compact due to intermolecular segregation of the polar P2VP arms [51] and due to good compatibility between the PS arms and the PPO matrix [52].

In this case, the contact angle of water on the membrane surface decreases; therefore, it may be concluded that the hybrid membranes become less hydrophobic than the pure PPO membranes.

3.1. Mass transfer of acetic acid and water

Transport of acetic acid and water through a membrane depend both on the membrane properties and the characteristics of test liquids. Table 2 shows some physicochemical properties of acetic acid and water. Water has lower boiling point, dynamic viscosity, and molecular size than those of acetic acid; molar volume of water is 3 times smaller than the corresponding parameter of acetic acid. On the contrary, the Hildebrand solubility parameter (δ) of acetic acid is significantly lower than that of water. The data on solubility parameters for different organic liquids can be used to predict solubility of a polymer in these liquids. According to the solubility theory [53], the less the difference between solubility parameters of a polymer and a liquid $|\Delta\delta|$, the better solubility of this liquid in the polymer. The δ value of PPO is equal to 18.2 $(J/cm^3)^{1/2}$ [39]. Hence, acetic acid solubility in the membranes should be preferential as compared to water.

The experiments involving sorption of acetic acid and water by PPO-0, PPO-1, PPO-3, and PPO-5 membranes were carried out in individual liquids according to the immersion method at 50 °C. Fig. 2 shows dependence of equilibrium sorption degree of acetic acid and water on star modifier content in the membrane. PPO-based membranes sorb acetic acid very well (this effect was expected when comparing solubility parameters), and the equilibrium sorption degree increases significantly with increasing percentage of P2VP-containing star modifier. The PPO-0 membrane practically does not sorb water. However, the presence of star macromolecules facilitates water sorption; as a result, the equilibrium sorption degree for PPO-5 membrane (the sample with the greatest modifier content) is equal to 5.6 g / 100 g of polymer. To summarize, the preferential sorption of acetic acid was established; an increase in the sorption activity of hybrid membranes with increasing modifier content was observed.

3.2. Pervaporation

Separation of acetic acid – water mixture was studied by pervaporation at 50 °C; the PPO-based membranes containing 0, 1, 3, and 5 wt% star modifier were used. All membranes were sufficiently permeable to water. Fig. 3 shows dependences of the total flux and the separation factor on water percentage in the feed. The total flux increases with increasing water content from 30 to 90 wt%, but the separation factor decreases in all cases. An increase in the star modifier content contributes to an increase in the flux and separation factor. The highest total flux and separation factor were revealed for PPO-5 hybrid membrane.

Table 1
Physical properties of membranes.

Membrane	Glass transition temperature, °C	Density, g cm^{-3}	Contact angle of water, °
PPO-0	176	1.057	86.4
PPO-1	196	1.059	83.1
PPO-3	203	1.062	81.7
PPO-5	204	1.064	80.3

Table 2
Physicochemical properties of liquids.

Liquid	Molecular weight, g mol^{-1}	Density, g cm^{-3}	Molar volume, cm^3 mol^{-1}	Viscosity, m·Pa·s	Solubility parameter, δ, $(J\ cm^{-3})^{1/2}$
Acetic acid	60.0	1.05	57.2	1.06	25.09
Water	18.0	0.99	18.0	0.89	42.89

To analyze transport properties of the membranes, the pervaporation processes should be described not only in terms of flux and separation factor, but also in terms of selectivity and permeability [49,54]. This approach allows normalizing the properties of membranes with respect to driving forces (partial vapor pressure) and makes it possible to reveal specific properties of the membrane–penetrant system. Permeabilities to individual liquids (water and acetic acid) and selectivity values ($\beta_{Water/HAc}$) were calculated for the original PPO-0 and hybrid membranes containing 1, 3, and 5 wt% of star molecules according to the procedures described by Baker et al. [49].

Fig. 4a shows the dependences of water and acetic acid permeability on water content in the feed. It is seen that introduction of star macromolecules into the membranes and increase in star modifier concentration lead to an increase in the permeability of small water molecules and decrease in the permeability of acetic acid that may be a result of increased sorption activity of hybrid membrane toward bulk acetic acid molecules. When the feed is enriched with acetic acid (water:acetic acid = 30:70), the PPO-5 membrane demonstrates the highest permeability; this result may be attributed to increased sorption activity of this sample toward acetic acid.

We should also take into account contribution of the polymer-analogous transformations in hybrid membranes into permeability improvement; these transformations occur during interaction between P2VP chains and acetic acid (Fig. 5) [55]. P2VP salt is soluble both in acetic acid and water, but it is not washed out from the membrane, since P2VP chains are covalently linked to the fullerene C_{60} core. Thus, sorption of acetic acid causes changes in the internal chemical structure of the transport channels, which facilitates mass transfer. Water is the more permeable component of the mixture due to smaller size of its molecules compared to that of acetic acid molecules.

The facilitated permeation of water molecules is reflected in the increased selectivity of the PPO-5 membrane. Fig. 4b shows the dependence of membrane selectivity ($\beta_{Water/HAc}$) on water content in the feed. In the absence of driving forces, the membrane selectivity also increases with increasing content of star macromolecules in the membrane.

3.3. Neutron scattering

Small-angle neutron scattering was used to obtain information about the structure of transport channels consisting of free volume elements and about the nature of connectivity between channels in modified membranes. The membranes were studied in the dry and swollen states after saturation with deuterated acetic acid, which has a strong contrast against the polymer matrix. Our aim was to study penetration of labeled small molecules of acetic acid into regions with different molecular packing densities in polymer matrices, depending on the amount of modifier (star macromolecules).

Embedding of star polymers into PPO matrix can be accompanied by segregation of the modifier molecules. Apparently, this process disturbs the original molecular packing of PPO matrix; this assumption is confirmed by the neutron scattering data obtained for dry films (Fig. 6). Increase in the content of star molecules up to 5 wt% leads to rise in the magnitude of cross section $\sigma(q)$ in the region of low momentum transfer values, $q < 0.3\ nm^{-1}$. This result indicates the formation of molecular ensembles at scales $R \geq 10$ nm (Fig. 6b). We estimated the size of density

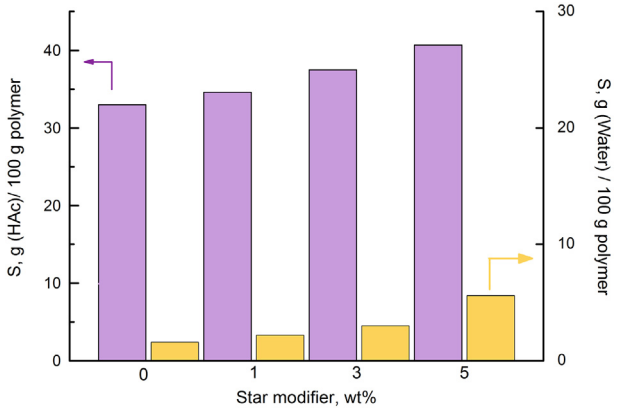

Fig. 2. Dependences of equilibrium sorption degrees of acetic acid (HAc) and water (S, g liquid/100 g polymer) on the content of star modifier in membranes, 50 °C.

inhomogeneities in PPO-5 using Guinier approximation for cross section [56],

$$\sigma(q) = \sigma_0 \exp[-(qR_q)^2/3] + B \quad (5)$$

where σ_0 is the forward cross section (the limit of $\sigma(q)$ at $q \to 0$), R_g is the gyration radius of inhomogeneities, and B is the contribution of incoherent scattering that appears mainly due to the presence of hydrogen in the sample. The fitting parameters of function (Eq. (5)) are listed in Table 3.

The cross section value $\sigma_0 = K_P^2(\Delta\rho/\rho)^2 V_C$ is determined by (*i*) the contrast factor of polymer (K_P) with respect to voids in the matrix, (*ii*) the characteristic value of density fluctuations ($\Delta\rho/\rho$) over the average density, and (*iii*) the correlation volume of a fluctuation $V_C = (4\pi/3)^{3/2}R_g^3 \sim 1 \cdot 10^4$ nm^3 related to its gyration radius $R_g \sim 11$ nm. The obtained

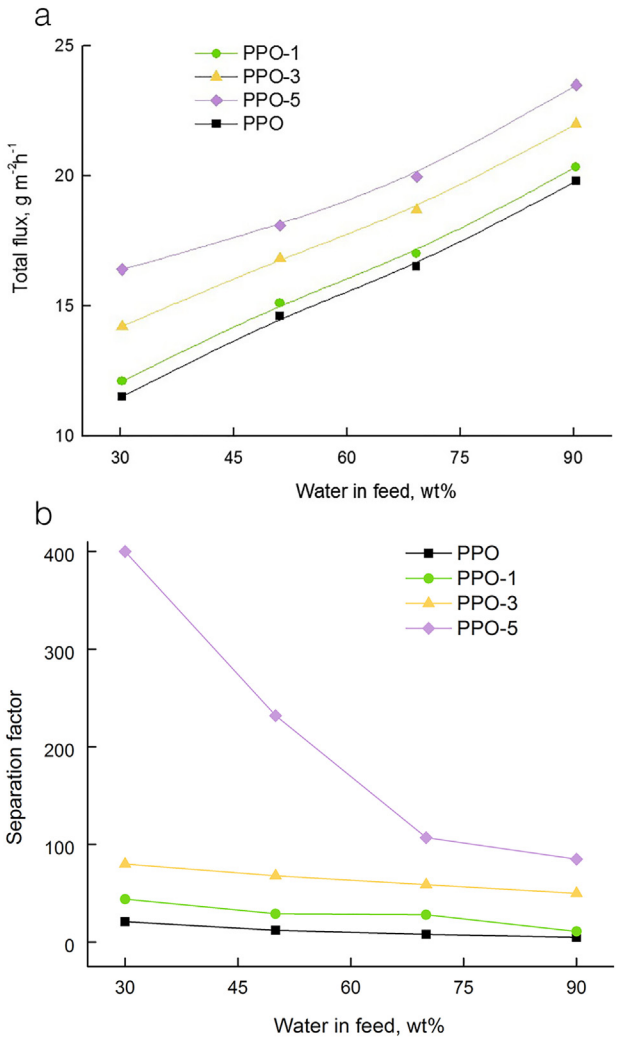

Fig. 3. Dependences of (a) total flux and (b) separation factor ($\alpha_{Water/HAc}$) on water concentration in the feed for pervaporation of water – acetic acid mixture, 50 °C.

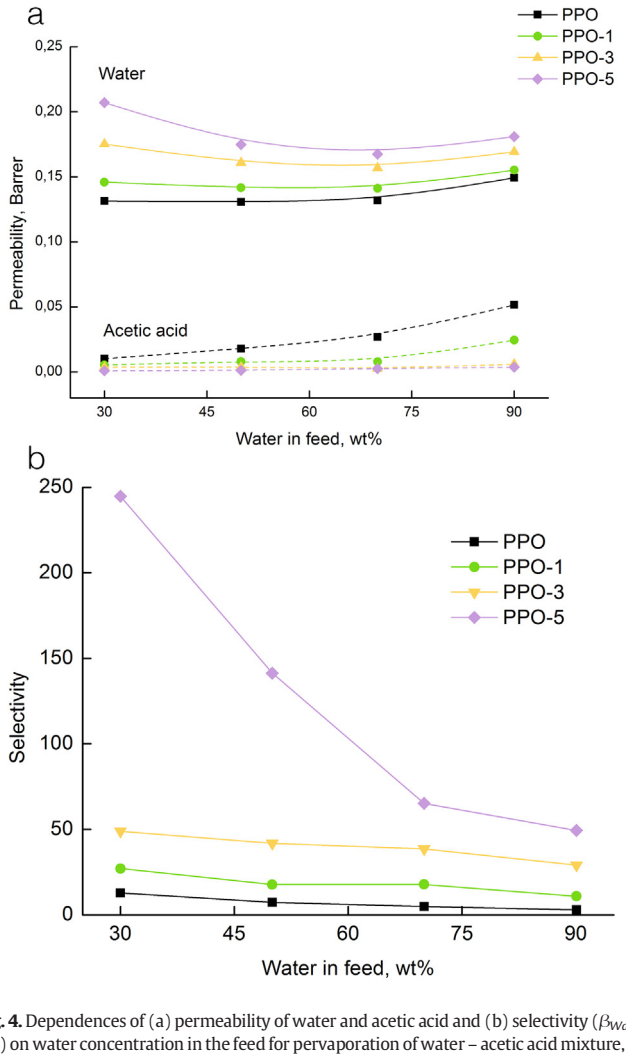

Fig. 4. Dependences of (a) permeability of water and acetic acid and (b) selectivity ($\beta_{Water/HAc}$) on water concentration in the feed for pervaporation of water – acetic acid mixture, 50 °C.

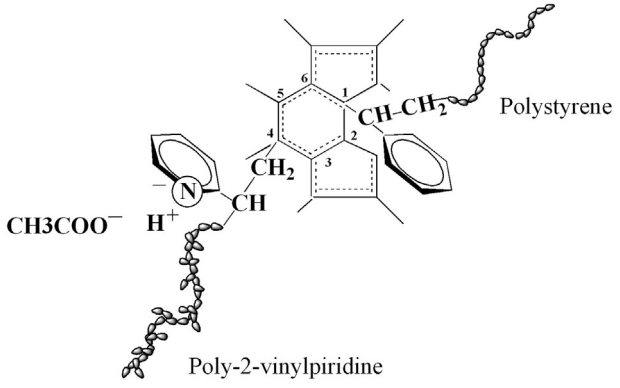

Fig. 5. Transformation of tertiary amino groups in the side fragments of P2VP into salt under the action of acetic acid. *The sites where PS and P2VP chains are attached to six-membered ring of C_{60} molecule are shown in the scheme.*

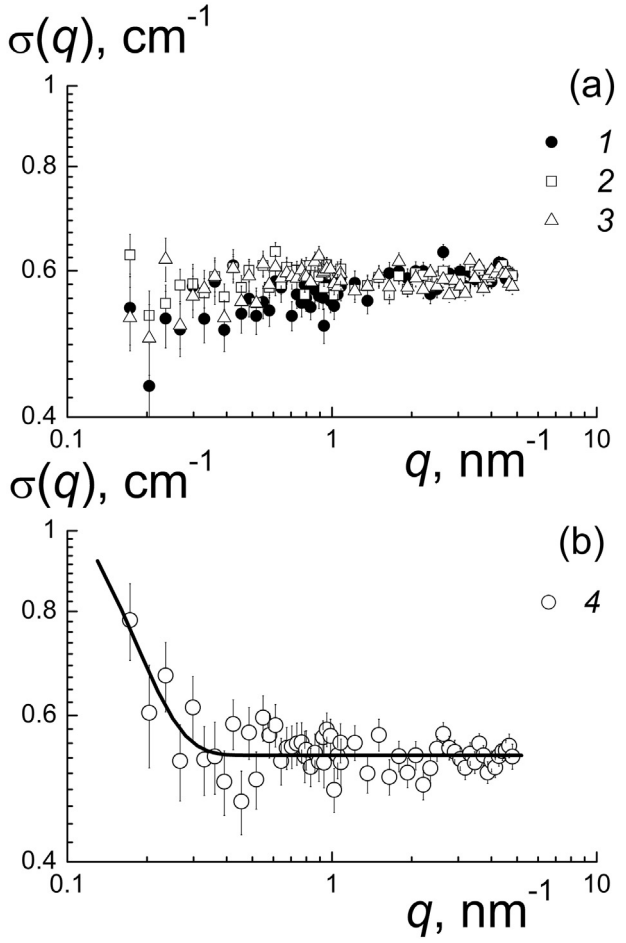

Fig. 6. Scattering cross section $\sigma(q)$ vs momentum transfer q for dry membranes: (1) PPO, (2) PPO-1, (3) PPO-2, and (4) PPO-5. The curve shows data fitting by function (Eq. (5)).

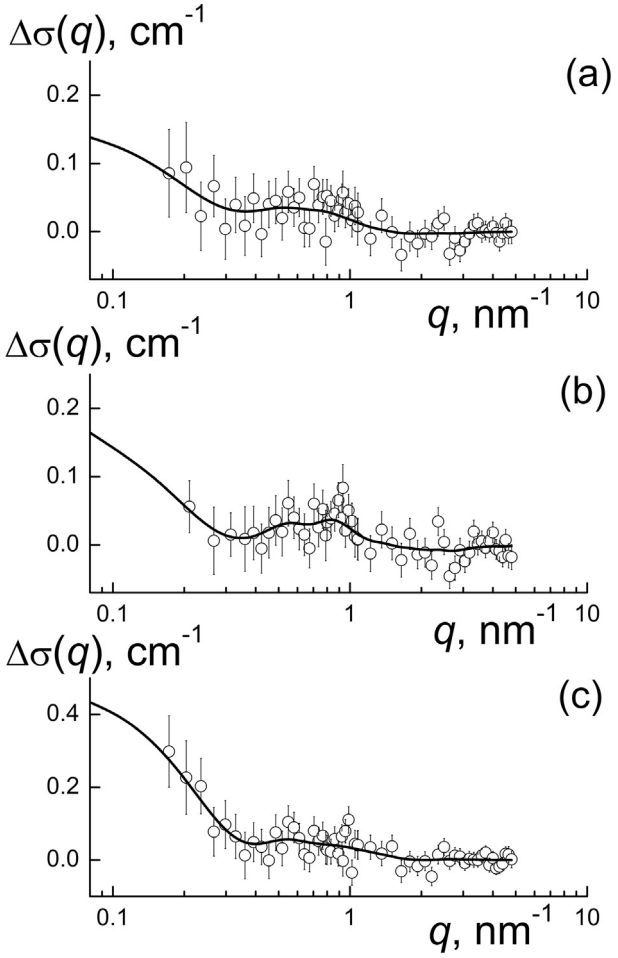

Fig. 7. Differential cross sections $\Delta\sigma(q)$ for dry membranes: (a) PPO-1, (b) PPO-3, (c) PPO-5.

parameters (Table 3) indicate relatively strong inhomogeneities in molecular packing ($\Delta\rho/\rho$ ~ 10%) that appeared due to the tendency of star macromolecules toward partial segregation. The size of these inhomogeneities (R_g ~ 11 nm) exceeds the gyration radius of a single star macromolecule in the case of Gaussian approximation of arms [57] ($R_{GG} = [(3f + 2)/f]^{1/2}R_{GA}$ ~ 4 nm, where f is the number of arms ($f = 12$) with gyration radius R_{GA}). At the same time, the observed size R_g ~ 11 nm is almost similar to the geometric radius of star molecule with completely stretched arms [58] ($R_{ST} = L_A$ ~ 17 nm, where $L_A = n{\cdot}b_u$ is the length of the arm composed of $n = 66$ units (the b_u length is equal to approximately 0.26 nm)). Note that these star macromolecules are regular structures; molecular weight of each arm is ~7000. As a first approximation, this molecule can be considered as a homogeneous sphere, and its gyration radius (R_{GSP} ~ 13 nm ~ R_g) approaches the experimentally determined size (R_g ~ 11 nm).

Analysis of the obtained data demonstrated that even at relatively low content (c = 5 wt%) of star-shaped molecules, the stars significantly disturb pristine molecular packing in the membrane matrix. Thus, transport properties of PPO can be changed substantially. It is noteworthy that such considerable inhomogeneities inside the PPO membrane appear due to overlapping of embedded star macromolecules, since their numerical concentration $N = c{\cdot}N_A/M_{ST}$ ~ $4{\cdot}10^{17}$ cm^{-3} defines average spacing between them (R_{int} ~ $N^{-1/3}$ ~ 14 nm ~ R_{GSP}). This distance is almost similar to gyration radius of the star molecule with stretched arms.

Table 3
Parameters of Guinier function (Eq. (5)) fitting the data for dry PPO-5 sample.

σ_0, cm^{-1}	R_g, nm	B, cm^{-1}
0.77 ± 0.69	11.2 ± 3.0	0.537 ± 0.003

Detailed analysis of structural features of membranes and relationship between membrane structure and content of star macromolecules was performed for differential cross sections (Fig. 7), $\Delta\sigma(q) = \sigma(q) - \sigma_m(q)$, where $\sigma_m(q)$ is the cross section for pure matrix. This approach enabled us to eliminate the contribution of inherent matrix inhomogeneities and to perform direct investigation of structural peculiarities of star molecules and their distribution in the PPO matrix. For this purpose, we used the scattering data to obtain the distributions of distances $G(R) = R^2\gamma(R)$ between scattering centers (repeating units, molecules and molecular clusters), where $\gamma(R)$ is the pair correlation function for these objects [56,59] (Fig. 8).

The scattering curves (Fig. 7) demonstrate a hump in the q range ~0.4–1.0 nm^{-1}. This feature reflects emergence of short-range order in the ensemble of objects arranged at characteristic distance R_q ~ $2\pi/q$ ~ 6–10 nm. Moreover, for samples with high concentration of modifier (5 wt%) the scattering becomes more intensive at $q < 0.3$ nm^{-1}, which indicates formation of clusters composed of such objects.

Detailed characterization and study of coordination of these objects were performed using the $G(R) = R^2\gamma(R)$ functions (Fig. 8).

All the spectra (Fig. 8) include the peak corresponding to the region of correlations inside star molecules, $R = 0$–4 nm. Position and width of this peak remain constant. Hence, size and conformation of molecules virtually do not change upon variation of their concentration. The integration of spectra over the peak region gave apparent gyration radii of the molecules, r_G ~ 1.6–1.8 nm (Fig. 9a). As expected, the r_G values are

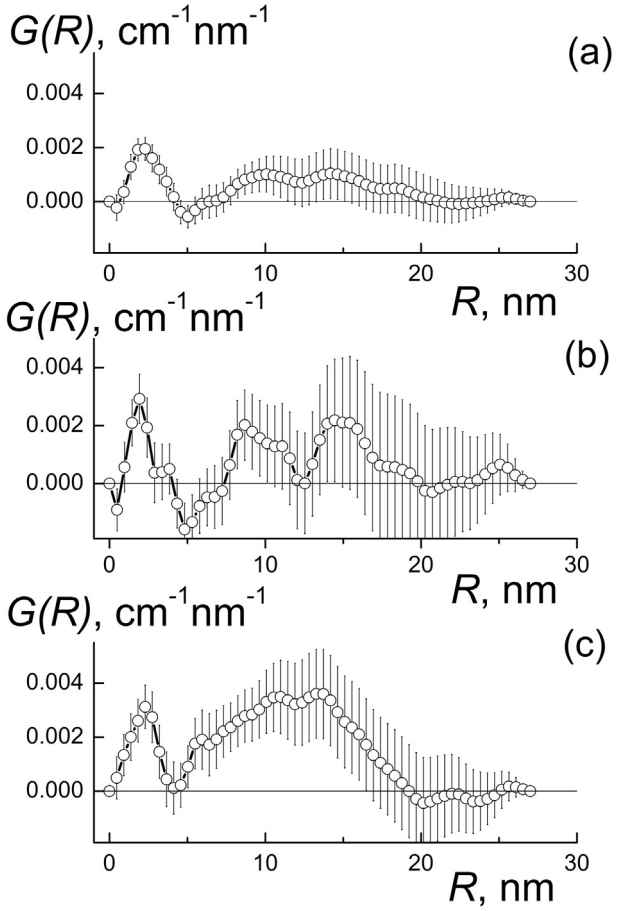

Fig. 8. Spectra of distances distributions $G(R)$ between scattering centers in the dry membranes: (a) PPO-1, (b) PPO-3, (c) PPO-5.

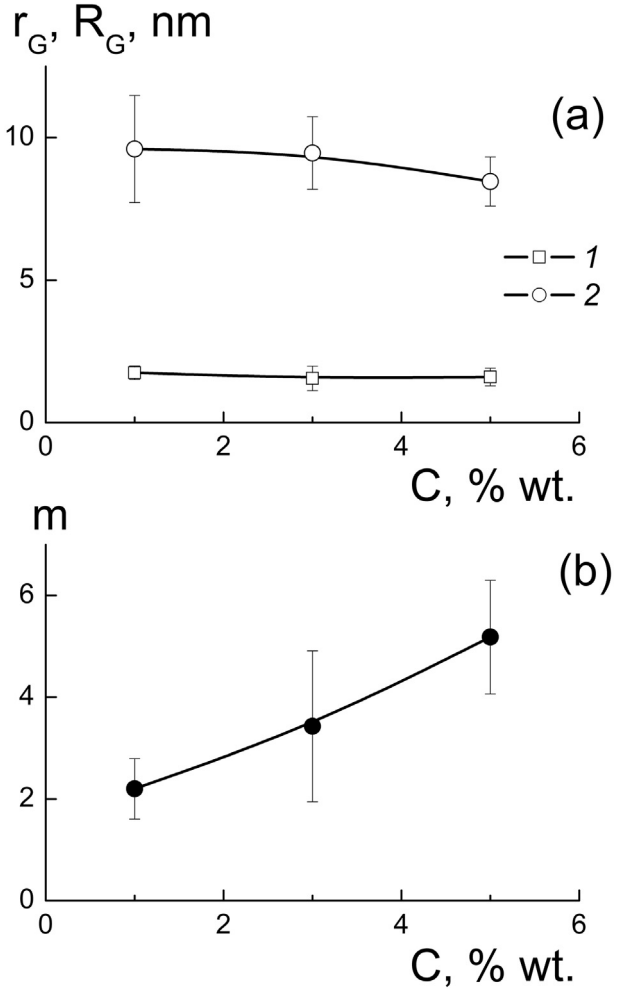

Fig. 9. (a) Dependences of gyration radii (r_G) of molecules (1) and aggregates (R_G) (2) on the concentration of star modifier; (b) dependence of aggregation number (m) on the concentration of star modifier. The data were obtained for dry membranes.

lower than the sizes of individual molecules which can be observed in dilute solutions. Obviously, the central cores of molecules are visible in the matrix. At larger scales (R = 5–25 nm) mutual correlations of star molecules manifest themselves as the peaks at R ~ 10 and 15 nm. They characterize molecular arrangement in the first and second coordination spheres around a given molecule. Their positions do not undergo any substantial changes with increasing star concentration. These are the spatial correlations of molecules contacting at the distances defined by their diameters. Discrete character of correlations becomes more distinct upon addition of the modifier; it is well pronounced at the star concentration of 3 wt%. Further addition of modifier leads to overlapping of molecules. Their interpenetration is evident from merging of peaks that form a wide hump in the range of distances R from 5 to 20 nm. The spectral integrals allowed us to find the gyration radii of aggregates (R_G ~ 9–10 nm) and aggregation numbers (m ~ 2–5) that depend on the content of star polymer in a composite (Table 4, Fig. 9).

According to the data obtained for dry samples (Fig. 9), the scales of structures at molecular and supramolecular levels remain stable, while the aggregation number is approximately linearly proportional to modifier content. Hence, the star molecules overlap progressively, and the overlapping causes structural changes in the areas around the aggregates. It was expected that these changes would be even more pronounced upon swelling of the membrane in acetic acid. The membranes were studied in swollen state after saturation with deuterated acetic acid. In swollen samples, the scattering increased due to penetration of the deuterated component into protonated matrix (Fig. 10).

As seen in Fig. 10, the swollen matrix demonstrates approximately constant cross section in the q range from 0.1 to 1.0 nm^{-1} (that is apparently attributed to predominant incoherent scattering due to the protons of polymers). The addition of 1 wt% of star macromolecules leads to increase in cross sections at $q < 0.7$ nm^{-1}, but the resulting values do not exceed the incoherent background. However, the samples containing 3 and 5 wt% of star modifier showed substantial enhancement of scattering, especially near the lower edge of q-range. The result is indicative of the presence of free volume regions that became filled by solvent in these samples.

To characterize the structures that induce scattering, we fitted the experimental data using the function including two coherent components and incoherent contribution,

$$\sigma(q) = \sigma_1 \exp\left[-(qR_{g1})^2/3\right] + \sigma_2\left[-(qR_{g2})^2/3\right] + B \quad (6)$$

The first component represents the scattering by the objects whose sizes are comparable to that of an individual star molecule. The second term is related to the scattering by larger objects (i.e., aggregates of

Table 4
Data for dry membranes: observed gyration radii of molecules and aggregates (r_G, R_G) and aggregation numbers (m) for hybrid membranes.

Membrane	r_G, nm	R_G, nm	m
PPO-1	1.75 ± 0.24	9.6 ± 1.9	2.2 ± 0.6
PPO-3	1.55 ± 0.43	9.5 ± 1.3	3.4 ± 1.5
PPO-5	1.60 ± 0.3	8.5 ± 0.9	5.2 ± 1.1

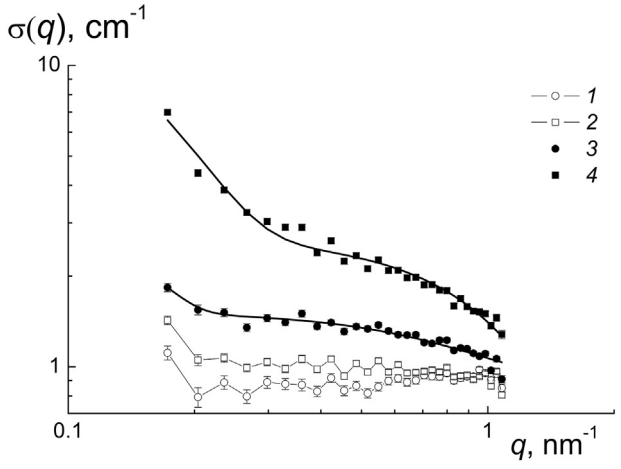

Fig. 10. Cross section $\sigma(q)$ vs momentum transfer q for swollen membranes: (1) PPO, (2) PPO-1, (3) PPO-3, and (4) PPO-5. The curves represent the fitting function (Eq. (6)).

molecules). These objects are characterized by the forward cross sections σ_1, σ_2 and the gyration radii R_{g1}, R_{g2} (Table 5).

Apparently, in the case of samples containing 3 and 5 wt% modifier, these small objects (gyration radii R_{g1} ~ 2 and 2.5 nm) are individual star molecules in the swollen state. Their size is higher (by 30% and 60%) than their dimensions in the dry state (r_G ~ 1.6–1.8 nm, Fig. 9a). Comparison of the data (Fig. 9, Table 5) showed that the size of aggregates is twice as large as that in the dry state for the membrane containing 3 wt% modifier (R_{g2}/R_G ~ 2.2). Hence, the regions occupied by these aggregates and the aggregate/matrix interfaces contain substantial free volume. On the contrary, the sample containing 5 wt% modifier is denser than other films. During swelling, it undergoes virtually similar expansion on the scale of single star molecules and on the scale of aggregates. The ratio between sizes of aggregates before and after swelling (R_{g2wet}/R_{g2dry} ~ 1.6) increases almost as much as that for single star molecules (by ~60%).

Although the regions in swollen membranes that contain aggregates of star molecules are relatively small (Table 5), it can be assumed that they play a crucial role in the pervaporation separation of water – acetic acid mixtures, since these domains demonstrate enhanced solubility and permeability.

3.4. Comparison of transport properties with literature data

The transport properties of the as-prepared hybrid PPO-5 membrane were compared with literature data for the case of separation of the acetic acid – water mixture containing 25–30 wt% water. Table 6 lists data on total flux and water concentration in feed and permeate that have been obtained by use of different polymer membranes [60–63]. The PPO-5 membrane shows high efficiency in the acid purification as compared to most published data, but it has moderate flux. The presented results indicate the promising application of PPO-5 as material for the dehydration of acetic acid, including as selective layer of composite or hollow fiber membranes.

Table 5
Fitting parameters of function (Eq. (6)) for swollen membrane samples: forward cross sections (σ_1, σ_2), gyration radii of molecules and aggregates (R_g).

Membrane	σ_1, cm^{-1}	σ_2, cm^{-1}	R_{g1}, nm	R_{g2}, nm
PPO-3	0.62 ± 0.02	27 ± 5	1.98 ± 0.04	21.0 ± 6.4
PPO-5	1.88 ± 0.04	22 ± 3	2.53 ± 0.11	13.3 ± 0.4

Table 6
Comparison of transport properties of membranes in pervaporation of the acetic acid – water mixture.

Membrane	T, °C	Water in feed, wt %	Water in permeate, wt%	Total flux, kg/m^2h	Separation factor	Ref.
NaAlg + 30% (HEC-g-AAm)	30	30	84.3	0.230	12.5	[60]
PEC/PW11	50	25	83.3	0.165	15	[61]
Zeolite DD3R	75	30	96.5	0.400	700	[62]
PANBA + (Na-MMT) nanofiller (0.5 wt %)	30	28	99.5	0.002	101	[63]
PPO-5	50	30	99.4	0.017	400	Present work

4. Conclusions

In this study, hybrid membranes were prepared from PPO modified with star macromolecules (which consist of fullerene C_{60} core with six attached PS arms and six P2VP arms); the membranes were successfully used for pervaporation dehydration of acetic acid – water mixture. The hybrid membranes exhibit impressive separation factor and acceptable flux value as compared with transport properties of known membranes. Notice also these data are obtained in the separation of acetic acid – water mixtures with high water concentration (30–90 wt%). The PPO-5 membrane shows separation factor of 400 and a total flux of 0.016 kg/m^2 h in the pervaporation of the mixture containing 30 wt% water at 50 °C. The aim of the majority of research works has been to dehydrate acetic acid in the mixtures with small water content (2–10 wt %). On the contrary, our hybrid membranes are promising objects for utilization of waste remaining after synthesis of acetic acid or other substances where acetic acid is involved. The hybrid membranes are very promising due to the fact that they include commercial PPO and very low amounts of star modifier (up to 5 wt%); the preparation method is extremely simple (mixing the solutions of components).

The use of small-angle neutron scattering in this work made it possible to obtain important information about the structure of membranes swollen in the deuterated acetic acid, which is close to the pervaporation conditions. The data on the neutron scattering in our hybrid membranes are indicative of non-uniform distribution of the embedded star macromolecules in the PPO matrix and reveal their aggregation at scales of several molecular diameters. The addition of star molecules results in their partial segregation when the aggregation number reaches ~2–5; finally, molecules overlap when concentration of star modifier is equal to 5 wt%. The star molecules introduced into the PPO matrix form fine supramolecular structures. The regions with increased solubility and permeability appear around these supramolecular structures due to transformation of P2VP chains into salt under the action of acetic acid. This effect leads to improvement of membrane transport properties.

Author contributions

Membrane preparation, physicochemical investigations, analysis of transport properties in pervaporation were carried out by Galina Polotskaya and Alexandra Pulyalina. Daria Rudakova also participated in membrane preparation and pervaporation tests. Vasily Lebedev and Gyula Török performed neutron scattering measurements. Ludmila Vinogradova was involved in scientific discussions and analysis of experimental data. All authors read and approved the final manuscript.

Funding

This research was financially supported by Russian Science Foundation (RSF), grant number 18-79-10116.

Declaration of competing interest

The authors declare that they have no known competing financial interests or personal relationships that could have appeared to influence the work reported in this paper.

References

[1] R.W. Baker, Membrane Technology and Applications, 3rd ed. John Wiley & Sons, Ltd, 2012https://doi.org/10.1016/S0958-2118(96)90133-0.

[2] Y. Yampolskii, I. Pinnau, B.D. Freeman, Materials Science of Membranes for Gas and Vapor Separation, John Wiley & Sons, Ltd, 2006https://doi.org/10.1002/047002903X.

[3] C. Chilev, F.D. Lamari, M. Dicko, E. Simeonov, Investigation of acetic acid dehydration by various methods, J. Chem. Technol. Metall. 51 (2016) 73–84.

[4] J.G. Crespo, C. Brazinha, Fundamentals of pervaporation, in: A. Basile, A. Figoli, M. Khayet (Eds.), Pervaporation, Vapour Permeation and Membrane Distillation: Principles and Applications, first ed.Woodhead Publishing 2015, pp. 3–17, https://doi.org/10.1016/C2013-0-16500-2.

[5] M.E. Dmitrenko, A.V. Penkova, A.I. Kuzminova, M. Morshed, M.I. Larionov, H. Alem, A.A. Zolotarev, S.S. Ermakov, D. Roizard, Investigation of new modification strategies for PVA membranes to improve their dehydration properties by pervaporation, Appl. Surf. Sci. 450 (2018) 527–537, https://doi.org/10.1016/j.apsusc.2018.04.169.

[6] H. Sardarabadi, S.M. Mousavi, E. Saljoughi, Removal of 2-propanol from water by pervaporation using poly(vinylidene fluoride) membrane filled with carbon black, Appl. Surf. Sci. 368 (2016) 277–287, https://doi.org/10.1016/j.apsusc.2016.01.227.

[7] J.-K. Wu, Ch.-Ch. Ye, T. Liu, Q.-F. An, Yi-Hu Song, K.-R. Lee, W.-S. Hung, C.-J. Gao, Synergistic effects of CNT and GO on enhancing mechanical properties and separation performance of polyelectrolyte complex membranes, Mater. Design. 119 (2017) 38–46, https://doi.org/10.1016/j.matdes.2017.01.056.

[8] M.E. Dmitrenko, A.V. Penlova, R.R. Atta, A.A. Zolotarev, T.V. Plisko, A.S. Mazur, N.D. Solovyev, S.S. Ermakov, The development and study of novel membrane materials based on polyphenylene isophthalamide - Pluronic F127 composite, Mater. Design. 165 (2019), 107596. https://doi.org/10.1016/j.matdes.2019.107596.

[9] H.S. Samanta, S.K. Ray, P. Das, N.R. Singha, Separation of acid–water mixtures by pervaporation using nanoparticle filled mixed matrix copolymer membranes, J. Chem. Technol. Biotechnol. 87 (2012) 608–622, https://doi.org/10.1002/jctb.2752.

[10] A. Banerjee, S.K. Ray, PVA modified filled copolymer membranes for pervaporative dehydration of acetic acid-systematic optimization of synthesis and process parameters with response surface methodology, J. Membr. Sci. 549 (2018) 84–100, https://doi.org/10.1016/j.memsci.2017.11.056.

[11] N. Alghezawi, O. Sanli, L. Aras, G. Asman, Separation of acetic acid–water mixtures through acrylonitrile grafted poly (vinyl alcohol) membranes by pervaporation, Chem. Eng. Process. 44 (2005) 51–58, https://doi.org/10.1016/j.cep.2004.03.007.

[12] N. Isiklan, O. Sanli, Permeation and separation characteristics of acetic acid/water mixtures through poly (vinyl alcohol-g-itaconic acid) membranes by pervaporation, evapomeation, and temperature-difference evapomeation, J. Appl. Polym. Sci. 93 (5) (2004) 2322–2333, https://doi.org/10.1002/app.20710.

[13] S.B. Kuila, S.K. Ray, Dehydration of acetic acid by pervaporation using filled IPN membranes, Sep. Purif. Technol. 81 (2011) 295–306, https://doi.org/10.1016/j.seppur.2011.07.033.

[14] H.K. Dave, K. Nath, Effect of temperature on pervaporation dehydration of water-acetic acid binary mixture, J. Sci. Ind. Res. 76 (2017) 217–222. http://nopr.niscair.res.in/handle/123456789/41046.

[15] N. Jullok, S. Darvishmanesh, P. Luis, B.V. Bruggen, The potential of pervaporation for separation of acetic acid and water mixtures using polyphenylsulfone membranes, Chem. Eng. J. 175 (2011) 306–315, https://doi.org/10.1016/j.cej.2011.09.109.

[16] R.Y.M. Huang, A. Moreira, R. Notarfonzo, Y. Xu, Pervaporation separation of acetic acid-water mixtures using modified membranes. I. Blended polyacrylic acid (PAA)-nylon 6 membranes, J. Appl. Polym. Sci. 35 (1988) 1191–1200, https://doi.org/10.1002/app.1988.070350506.

[17] R.Y.M. Huang, Y.F. Xu, Pervaporation separation of acetic acid-water mixtures using modified membranes. Part II. Gammaray-induced grafted polyacrylic acid (PAA)-nylon 6 membranes, J. Membr. Sci. 43 (2–3) (1989) 143–148, https://doi.org/10.1016/S0376-7388(00)85093-0.

[18] Y. Wang, T. S. Chung, M. Gruender, Sulfonated polybenzimidazole membranes for pervaporation dehydration of acetic acid, J. Membr. Sci. 415 (2012) 486–495. doi: 10.1016./j.memsci.2012.05.035.

[19] S.-Y. Lu, H.-Y. Huang, K.-H. Wu, Silicalite/poly(dimethylsiloxane) nanocomposite pervaporation membranes for acetic acid/water separation, J. Mater. Res. 16 (11) (2001) 3053–3059, https://doi.org/10.1557/JMR.2001.0422.

[20] A.A. Kittur, S.M. Tambe, S.S. Kulkarni, M.Y. Kariduraganavar, Pervaporation separation of water–acetic acid mixtures through NaY zeolite-incorporated sodium alginate membranes, J. Appl. Polym. Sci. 94 (9) (2004) 2101–2109, https://doi.org/10.1002/app.21149.

[21] S.S. Kulkarni, S.M. Tambe, A.A. Kittur, M.Y. Kariduraganavar, Preparation of novel composite membranes for the pervaporation separation of water–acetic acid mixtures, J. Membr. Sci. 285 (2006) 420–431, https://doi.org/10.1016/j.memsci.2006.09.021.

[22] M.E. Dmitrenko, A.V. Penkova, A.I. Kuzminova, S.S. Ermakov, D. Roizard, Development and investigation of mixed-matrix PVA-fullerenol membranes for acetic acid dehydration by pervaporation, Sep. Purif. Technol. 187 (2017) 285–293, https://doi.org/10.1016/j.seppur.2017.06.061.

[23] A.B. Samit, K. Ray, PVA modified filled copolymer membranes for pervaporative dehydration of acetic acid-systematic optimization of synthesis and process parameters with response surface methodology, J. Membr. Sci. 549 (2018) 84–100, https://doi.org/10.1016/j.memsci.2017.11.056.

[24] T. Sano, S. Ejiri, K. Yamada, Y. Kawakami, H. Yanagishita, Separation of acetic acid-water mixtures by pervaporation through silicalite membrane, J. Membr. Sci. 123 (2) (1997) 225–233, https://doi.org/10.1016/S0376-7388(96)00224-4.

[25] T. Tsuru, T. Shibata, J. Wang, H.R. Lee, M. Kanezashi, T. Yoshioka, Pervaporation of acetic acid aqueous solutions by organosilica membranes, J. Membr. Sci. 421 (2012) 25–31, https://doi.org/10.1016/j.memsci.2012.06.012.

[26] S.P. Kusumocahyo, M. Sudoh, Pervaporation of acetic acid-water mixture using silica membrane prepared by sol-gel method, J. Eng. Technol. Sci. 48 (1) (2016) 99–110, https://doi.org/10.5614/j.eng.technol.sci.

[27] X. Kai, J. Zhenqi, F. Bo, H. Aisheng, A graphene oxide layer as an acid-resisting barrier deposited on a zeolite LTA membrane for dehydration of acetic acid, RSC Adv. 6 (28) (2016) 23354–23359, https://doi.org/10.1039/C6RA00802J.

[28] K.S.V. Krishna Rao, B. Vijaya Kumar Naidu, M.C.S. Subha, M. Sairam, N.N. Mallikarjuna, T.M. Aminabahvi, Novel carbohydrate polymeric blend membranes in pervaporation dehydration of acetic acid, Carbohydr. Polym. 66 (2006) 345–351, https://doi.org/10.1016/j.carbpol.2006.03.024.

[29] S.D. Bhat, T.M. Aminabhavi, Pervaporation-aided dehydration and esterification of acetic acid with ethanol using 4A zeolite-filled cross-linked sodium alginate-mixed matrix membranes, J. Appl. Polym. Sci. 113 (157–168) (2009) 157–168, https://doi.org/10.1002/app.29545.

[30] W. Zhang, Y. Xu, Z. Yu, Sh. Lu, X. Wang, Separation of acetic acid/water mixtures by pervaporation with composite membranes of sodium alginate active layer and microporous polypropylene substrate, J. Membr. Sci. 451 (2014) 135–148, https://doi.org/10.1016/j.memsci.2013.09.027.

[31] S. Moulik, Sh. Nazia, B. Vani, S. Sridhar, Pervaporation separation of acetic acid/water mixtures through sodium alginate/polyaniline polyion complex membrane, Sep. Purif. Technol. 170 (2016) 30–39, https://doi.org/10.1016/j.seppur.2016.06.027.

[32] G. Chowdhury, B. Kruczek, T. Matsuura, Polyphenylene oxide and modified polyphenylene oxide membranes: gas, vapor and liquid separation, J. Membr. Sci. 217 (1–2) (2003) 299–300, https://doi.org/10.1016/S0376-7388(03)00124-8.

[33] M. Khayet, J.P.G. Villaluenga, M.P. Godino, J.I. Mengual, B. Seoane, K.C. Khulbe, T. Matsuura, Preparation and application of dense poly(phenylene oxide) membranes in pervaporation, J. Colloid Interface Sci. 278 (2004) 410–422, https://doi.org/10.1016/j.jcis.2004.06.021.

[34] G.A. Polotskaya, A.V. Penkova, A.M. Toikka, Fullerene-containing polyphenylene oxide membranes for pervaporation, Desalination 200 (1–3) (2006) 400–402, https://doi.org/10.1016/j.desal.2006.03.347.

[35] G.A. Polotskaya, A.V. Penkova, A.M. Toikka, Z. Pientka, L. Brozova, M. Bleha, Transport of small molecules through polyphenylene oxide membranes modified by fullerene, Sep. Sci. Technol. 42 (2) (2007) 333–347, https://doi.org/10.1080/01496390600999796.

[36] A.V. Penkova, G.A. Polotskaya, A.M. Toikka, Pervaporation composite membranes for ethyl acetate production, Chem. Eng. Process.: Process Intensification 87 (2015) 81–87, https://doi.org/10.1016/j.cep.2014.11.015.

[37] G.A. Polotskaya, N.V. Avagimova, A.M. Toikka, N.V. Tsvetkov, A.A. Lezov, I.A. Strelina, I.V. Gofman, Z. Pientka, Optical, mechanical, and transport studies of nanodiamonds/poly(phenylene oxide) composites, Polym. Compos. 39 (11) (2018) 3952–3961, https://doi.org/10.1002/pc.24437.

[38] M. Khayet, J.P.G. Villaluenga, J.L. Valentini, M.A. Lopez-Manchado, J.I. Mengual, B. Seoane, Filled poly(2,6-dimethyl-1,4-phenylene oxide) dense membranes by silica and silane modified silica nanoparticles: characterization and application in pervaporation, Polymer 46 (2005) 9881–9891, https://doi.org/10.1016/j.polymer.2005.07.081.

[39] G.A. Polotskaya, E.L. Krasnopeeva, L.M. Kalyuzhnaya, N.N. Saprykina, L.V. Vinogradova, Mixed matrix membranes with hybrid star-shaped macromolecules for mono- and dihydric alcohols pervaporation, Sep. Purif. Technol. 143 (2015) 192–200, https://doi.org/10.1016/j.seppur.2015.02.002.

[40] G.A. Polotskaya, A.Y. Pulyalina, V.A. Rostovtseva, A.M. Toikka, N.N. Saprykina, L.V. Vinogradova, Effect of polystyrene stars with fullerene C_{60} cores on pervaporation properties of poly(phenylene oxide) membrane, Polym. Int. 65 (2016) 407–414, https://doi.org/10.1002/pi.5069.

[41] A. Pulyalina, D. Porotnikov, D. Rudakova, I. Faykov, I. Chislova, V. Rostovtseva, L. Vinogradova, A. Toikka, G. Polotskaya, Advanced membranes containing star macromolecules with C_{60} core for intensification of propyl acetate production, Chem. Eng. Res. Des. 135 (2018) 197–206, https://doi.org/10.1016/j.cherd.2018.05.034.

[42] V. Lebedev, Y. Kulvelis, D. Orlova, E. Krasnopeeva, V. Shamanin, L. Vinogradova, Neutron studies of composites of poly(phenylene oxide) modified by hybrid star-shaped fullerene-containing macromolecules, Macromol. Symp. 348 (1) (2015) 54–62, https://doi.org/10.1002/masy.201400165.

[43] V.T. Lebedev, Y. Kul'velis, D.N. Orlova, V.V. Shamanin, L.V. Vinogradova, Structural features of films based on star-shaped fullerene-containing polystyrenes: small-angle neutron-scattering study, Polym. Sci. 58 (5) (2016) 697–709, https://doi.org/10.1134/S0965545X16050114.

[44] A.Y. Pulyalina, V.A. Rostovtseva, Z. Pientka, L.V. Vinogradova, G.A. Polotskaya, Hybrid gas separation membranes containing star-shaped polystyrene with the fullerene (C60) core, Pet. Chem. 58 (4) (2018) 296–303, https://doi.org/10.1134/S0965544118040084.

[45] L.V. Vinogradova, O.V. Ratnikova, E.A. Butorina, H.-J.P. Adler, Grafting of fullerene C_{60} by poly(2-vinylpyridine) chains in anionic polymerization processes, Polym. Sci. Ser. A. 47 (9) (2005) 920–927, 920-926 https://doi.org/10.1021/ma961671d.

[46] L.V. Vinogradova, Star-shaped polymers with the fullerene C_{60} branching center, Russ. Chem. Bull. 61 (2012) 907–925, https://doi.org/10.1007/s11172-012-0135-1.

[47] L.V. Vinogradova, Anionic methods for synthesis of star polymers, Russ. J. Appl. Chem. 83 (2010) 351–378, https://doi.org/10.1134/S1070427210030018.

[48] V.F. Sears, Neutron scattering lengths and cross sections, Neutron News 3 (3) (1992) 26–37, https://doi.org/10.1080/10448639208218770.
[49] R.W. Baker, J.G. Wijmans, Y. Huang, Permeability, permeance and selectivity: a preferred way of reporting pervaporation performance data, J. Membr. Sci. 348 (2010) 346–352, https://doi.org/10.1016/j.memsci.2009.11.022.
[50] D.F. Othmer, S.J. Silvis, A. Spiel, Composition of vapors from boiling binary solutions: pressure equilibrium still for studying water - acetic acid system, Ind. Eng. Chem. 44 (1952) 1864–1872, https://doi.org/10.1021/ie50512a041.
[51] P.N. Lavrenko, I.P. Kolomiets, O.V. Ratnikova, L.V. Vinogradova, Hydrodynamic and electrooptical properties of star-shaped heteroarm fullerene (C60)-containing polymers in solutions, Polym. Sci. Ser. A. 50 (2008) 848–853, https://doi.org/10.1134/S0965545X0808004X.
[52] D.R. Paul, S. Newman (Eds.), Polymer Blends, first ed., V.1, Academic Press, 1978.
[53] M. Belmares, M. Blanco, W.A. Goddard, R.B. Ross, G. Caldwell, S.H. Chou, J. Pham, P.M. Olofson, C. Thomas, Hildebrand and Hansen solubility parameters from molecular dynamics with applications to electronic nose polymer sensors, J. Comput. Chem. 25 (2004) 1814–1826, https://doi.org/10.1002/jcc.20098.
[54] W.F. Guo, T.S. Chung, T. Matsuura, Pervaporation study on the dehydration of aqueous butanol solutions: a comparison of flux vs. permeance, separation factor vs. selectivity, J. Membr. Sci. 245 (2004) 199–210, https://doi.org/10.1016/j.memsci.2004.07.025.
[55] B. Vollmert, Polymer Chemistry, Springer, 1973https://doi.org/10.1007/978-3-642-65293-6.
[56] L.A. Feigin, D.I. Svergun, in: G.W. Taylor (Ed.), Structure Analysis by Small-Angle X-Ray and Neutron Scattering, Plenum press, New York and London, 1987.
[57] M. Rawiso, De l'intensité à la structure en physico-chimie des polymères, J. de Phys. IV. 9 (1999) 174–195, https://doi.org/10.1051/jp4:1999110.
[58] M. Daoud, J.P. Cotton, Star shaped polymers: a model for the conformation and its concentration dependence, J. de Phys. 43 (1982) 531–538, https://doi.org/10.1051/jphys:01982004303053100.
[59] D.I. Svergun, Determination of the regularization parameter in indirect-transform methods using perceptual criteria, J. Appl. Crystallogr. 25 (1992) 495–503, https://doi.org/10.1107/S0021889892001663.
[60] K.S.V. Krishna Rao, B. Vijaya Kumar Naidu, M.C.S. Subha, M. Sairam, N.N. Mallikarjuna, T.M. Aminabahvi, Novel carbohydrate polymeric blend membranes in pervaporation dehydration of acetic acid, Carbohydr. Polym. 66 (2006) 345–351, https://doi.org/10.1016/j.carbpol.2006.03.024.
[61] J.H. Chen, J.Z. Zheng, Q.L. Liu, H.X. Guo, W. Weng, S.X. Li, Pervaporation dehydration of acetic acid using polyelectrolytes complex (PEC)/11-phosphotungstic acid hydrate (PW11) hybrid membrane (PEC/PW11), J. Membr. Sci. 429 (2013) 206–213, https://doi.org/10.1016/j.memsci.2012.11.038.
[62] Y. Zhang, X. Qiu, Z. Hong, P. Du, Q. Song, X. Gu, All-silica DD3R zeolite membrane with hydrophilic-functionalized surface for efficient and highly-stable pervaporation dehydration of acetic acid, J. Membr. Sci. 581 (2019) 236–242, https://doi.org/10.1016/j.memsci.2019.03.061.
[63] H.S. Samanta, S.K. Ray, P. Das, N.R. Singha, Separation of acid–water mixtures by pervaporation using nanoparticle filled mixed matrix copolymer membranes, J. Chem. Technol. Biotechnol. 87 (2012) 608–622, https://doi.org/10.1002/jctb.2752.